

Peripheral Blood-Derived Endothelial Progenitor Cells Enhance Vertical Bone Formation

Hadar Zigdon-Giladi, DMD, PhD;^{*,†,**,§} Tova Bick, PhD;[§] Elise F. Morgan, PhD;^{‡‡} Dina Lewinson, PhD;[‡] Eli E. Machtei, DMD^{†,‡‡}

ABSTRACT

Background: This study presents a novel cell-based approach for extra-cortical bone regeneration.

Objective: To enhance vertical bone formation by combining guided bone regeneration and transplantation of peripheral blood-derived endothelial progenitor cells (EPCs) in a rat calvaria model.

Materials and Methods: EPCs were isolated from peripheral blood of inbred rats. Gold domes (7 mm radius, 5 mm height) were filled with β -tricalcium phosphate (β TCP) mixed with 5×10^5 EPC. Domes filled with β TCP served as control (CNT). Rats were sacrificed after 3 months. Vertical bone augmentation was analyzed using histology, histomorphometry, and microcomputed tomography (μ CT).

Results: In all rats, hard tissue filled the space under the dome. Histomorphometric analysis revealed that EPC transplantations doubled vertical bone height (EPC 4.04 ± 0.22 mm vs CNT 2.29 ± 0.22 mm, $p \leq .001$). EPC also caused ~50% increase in bone area fraction (EPC $47.3 \pm 3.1\%$ vs CNT $31.1 \pm 2.7\%$, $p \leq .003$). μ CT results also showed that bone volume fraction (BV/TV) was higher in EPC group ($p = .0169$). In both groups, BV/TV declined from the bottom to the top of the samples. No differences in tissue mineral density were found between EPC and CNT groups.

Conclusion: EPC transplantation significantly improved bone formation especially in the areas that are remote from the original bone.

KEY WORDS: bone regeneration, cell therapy, microcomputed tomography, peripheral blood-derived endothelial progenitor cells, tissue engineering

INTRODUCTION

Alveolar bone loss constitutes a major challenge for placement of dental implants. Restoring the lost bone is crucial to allow dental implant placement and to

rehabilitate patient's function, phonetics, and aesthetic. Currently, the techniques available for vertical bone augmentation include bone blocks (autologic/allogenic or xenogenic), distraction osteogenesis, and guided bone regeneration (GBR). Autologous bone graft is the gold standard for vertical bone augmentation.¹ However, this technique has many disadvantages, such as donor site morbidity, postsurgical pain, nerve and soft-tissue injuries, increased intraoperative time, and deficiencies in the quality and quantity of available bone.² Moreover, the majority of the osteogenic cells in the harvested graft do not survive the harvesting and transplantation procedures.³ Alternatively, GBR is a common and relatively predictable procedure for intrabony defects⁴; however, vertical extra-cortical bone augmentation by GBR is very limited and still unpredictable with minimal vertical bone gain.^{5,6} A comprehensive review that compared different surgical techniques for vertical bone augmentation concluded that while it is possible to vertically augment bone with different techniques, the

*Department of Periodontology, School of Graduate Dentistry, Rambam Health Care Campus, Haifa, Israel; †Department of Periodontology, School of Graduate Dentistry, Rambam Health Care Campus, Haifa, Israel; ‡Research Institute for Bone Repair, Rambam Health Care Campus, Haifa, Israel; §Research Institute for Bone Repair, Rambam Health Care Campus, Haifa, Israel; ¶Research Institute for Bone Repair, Rambam Health Care Campus, Haifa, Israel; **The Rappaport Family Faculty of Medicine, Technion – Israel Institute of Technology, Haifa, Israel; ††The Rappaport Family Faculty of Medicine, Technion – Israel Institute of Technology, Haifa, Israel; ‡‡Department of Mechanical Engineering, Boston University, Boston, MA, USA

Reprint requests: Dr. Hadar Zigdon-Giladi, Research Institute for Bone Repair, Rambam Health Care Campus, 8, Ha'aliya st., Bat-Galim, P.O. Box 9602, Haifa 31096, Israel; e-mail: hadar@tx.technion.ac.il

© 2013 Wiley Periodicals, Inc.

DOI 10.1111/cid.12078

frequency of complications and failures of the augmentation procedures is still too high (well over 20%) to recommend a widespread use of such procedures.⁷

During the postnatal period, bone is constantly being remodeled. Following injury, bone regeneration may also occur, owing to the activities of host stem cells. Basic multicellular units that participate in bone remodeling and regeneration consist of osteoclasts, osteoblasts, osteocytes, and lining cells that share an intimate relationship with blood vessels.⁸ However, in cases of severe bone loss, the inadequate supply of osteoprogenitor cells and limited blood supply restrict bone regeneration. A tissue engineering approach that combines stem cells and osteoconductive scaffold transplantation might enhance bone regeneration. This approach offers several potential benefits including the lack of donor site morbidity, less technical variability, and the ability to closely recapitulate normal craniofacial development and repair.^{9,10}

Cell-based therapies used until now involved fresh bone marrow (bm) or ex vivo expanded mesenchymal stem cells (MSCs), usually combined with scaffolds. MSCs contribute to the maintenance of various tissues, especially bone, in adults. MSCs were first described by Friedenstein¹¹ and can be isolated from adult's bm, placenta, umbilical cord blood, or adipose tissue.¹² MSCs adhere to culture plates and demonstrate a fibroblast-like phenotype and proliferation potential. In vivo and in vitro studies showed that MSC can be transformed into bone, cartilage, adipose, muscle, and tendon.¹² In animal models, transplantation of MSC formed ectopic bone and improved healing of bone defects.^{13,14} In clinical trials, MSCs regenerate bone in nonunion long bone defects,¹⁵ in children with osteogenesis imperfecta¹⁶ and in maxillofacial surgeries.¹⁷ Although promising clinical results have been achieved,¹⁵⁻¹⁷ the necessity of anesthesia and an invasive manipulation requiring a minimum of two surgeries is a disadvantage. Therefore, other sources for osteogenic progenitor cells are needed. The presence of circulating progenitor cells with osteogenic potential was described by Kuznetsov and colleagues.¹⁸ Peripheral blood contains multipotential progenitor cells that are able to differentiate into cells expressing endothelial markers that are defined as endothelial progenitor cells (EPCs) and into cells expressing osteogenic markers.^{19,20} EPCs were shown to participate in postnatal neovascularization, angiogenesis, vascular repair, and vasculoprotection and to home and participate in

the revascularization of ischemic tissues.²¹⁻²³ In the last decade, several research groups transplanted EPC into critical size defects in long bones, with promising results.²⁴⁻²⁶

Based on these observations, we hypothesized that transplantation of EPC seeded on scaffold under a rigid physical barrier, according to the principles of the GBR technique, will enhance vertical extra-cortical bone augmentation.

MATERIALS AND METHODS

Isolation and Expansion of Peripheral Blood-Derived EPC

Pooled peripheral blood (20–30 mL) was obtained from the heart of five male Lewis inbred rats (300 g). Blood was collected into a sterile heparinized tubes and EPCs were isolated as previously described for sheep EPC.²⁴ Briefly, blood was diluted 1:1 with phosphate buffered saline (PBS). Mononuclear cells (MNCs) were isolated with density gradient centrifugation (LymphoprepTM, Axis-Shield, Oslo, Norway) and pelleted cells were resuspended in endothelial basal medium (EBM-2) containing 20% heat inactivated fetal bovine serum and penicillin-streptomycin (Biological Industries Ltd, Beit Haemek, Israel) and supplemented with endothelial growth medium (EGM-2MV SingleQuote; Clonetics, Cambrex Bio Science, Walkersville, MD, USA) that includes the following: vascular endothelial growth factor (VEGF), fibroblast growth factors (FGF)-2, epidermal growth factor (EGF), insulin growth factor (IGF)-1, and ascorbic acid. Cells were seeded on six-well plates coated with 5 µg/cm² of fibronectin (Biological Industries Ltd) and grown at 37°C with humidified 95% air/5% CO₂. After 4 days of culture, nonadherent cells were discarded by gentle washing with PBS, and fresh medium was applied. The attached cells were continuously cultured with complete EGM-2 medium. Cells were fed three times per week and were split when reached ~80% confluent by brief trypsinization using 0.5% trypsin in 0.2% EDTA (Biological Industries Ltd).

EPC Characterization

Flow Cytometry (FACS) Analysis. EPCs were characterized by fluorescence-activated cell sorting (FACS) analysis using fluorescein isothiocyanate (FITC)-labeled antibodies specific for CD90, CD45, CD44, CD31 (mouse anti-rat Serotec, Kidlington, UK; BioLegend,

San Diego, CA, USA), and CD34 (rabbit polyclonal antibody, Bioss, Woburn MA, USA). For this analysis, 5×10^5 cells at passages 3 to 5 suspended in PBS were incubated with the antibodies for 30 minutes in the dark at room temperature according to the manufacturers' recommendations. Negative controls used were mouse IgG1 (Serotec) or rabbit IgG FITC isotypes (Jackson, Baltimore Pike, PA, USA). Following washings three times with PBS, cells were resuspended in 0.5 mL of PBS and analyzed using FACScan and CellQuest software (Becton Dickinson & Co., Franklin Lakes, NJ, USA).

Tube Formation on Matrigel. EPCs were seeded on Matrigel-coated plates²⁴ and cultured with EGM-2MV and followed for 5 days for formation of clusters and tubes. Briefly, 250 μ L of growth factor-reduced Matrigel (BD Biosciences Discovery Labware, Bedford, MA, USA) was added per well of a 24-well plate and allowed to polymerize at 37°C for at least 30 minutes. The 5×10^4 adherent cells were suspended in 300 μ L EGM-2MV medium and seeded onto Matrigel. The cells were incubated at 37°C with humidified 95% air/5% CO₂. The tube networks were observed with an Olympus inverted microscope (Olympus, CKX41, Olympus, Tokyo, Japan).

Coating of β -Tricalcium Phosphate (β TCP) with Fibronectin

In accordance with the results obtained in our previous study,²⁷ β TCP was used as scaffold for the present study. To enable attachment of cells, on the day of surgery, β TCP granules (Poresorb-TCP®, Lasak Ltd, Prague, Czech Republic) were coated with fibronectin as described by Seebach and colleagues.²⁵ Briefly, for each rat, 0.2-g β TCP granules were placed as a dense monolayer in each well of a 24-well plate, mixed with 50 μ g fibronectin and incubated for 30 minutes in 37°C.

Cell Transplantation

The experimental procedures were approved by the committee for the supervision of animal experiments at the Faculty of Medicine, Technion (I.I.T.) no. IL0080109.

Male Lewis rats (300 g) were anesthetized by intramuscular injection of 100 mg/kg body weight (bw) ketamin (Ketaset, Fort Dodge, IA, USA) and 5 mg/kg bw Xylazine (Eurovet, Cuijk, Holland). The 50 mg/kg bw cephalixin (Norbrook Laboratories, Ireland) and

0.3 mg/kg bw buprenorphine (Vetamarket, Israel) were injected subcutaneous preoperatively and 3 days postoperation. Surgical procedure was performed as previously described.^{27,28} Briefly, a U-shaped incision served to raise a full-thickness skin flap and exposure of the parietal bone. Five perforations (1 mm diameter) of the cortical bone were performed to allow passage of blood, cells, and nutrients from the bm into the space under the dome. Just prior to transplantation, 5×10^5 EPCs suspended in 50 μ L EBM-2 ($n = 8$) or 50 μ L EBM-2 (control [CNT] [$n = 8$]) were mixed with 0.2 g fibronectin-coated β TCP particles and filled rigid gold domes (7 mm radius, 5 mm height). The domes were secured to the calvarium using fixation screws. The flaps were repositioned and sutured. Each rat was kept in a separate cage and fed rat chow and water ad libitum for 3 months. Then, rats were sacrificed by CO₂ asphyxiation and the domes were removed. The part of the calvarium surrounding the regenerated area was sawed out and specimens were fixed immediately in 10% neutral buffered formalin (NBF) for 2 days and analyzed by microcomputed tomography (μ CT) and by histomorphometry.

μ CT Scanning

All specimens were scanned in a desktop μ CT system (Scanco μ 40, Brütisellen, Switzerland) at 80 V and 80 μ A, with a 200-ms integration time. The image resolution was 20 μ m/voxel. Each scan included a phantom containing regions of different hydroxyapatite densities for conversion of attenuation to mineral density (in mg HA/cm³). Specimen-specific thresholds to identify the TCP and, separately, the mineralized tissue were chosen by identifying the peak in the attenuation histogram that corresponded to mineralized tissue and then setting the upper and lower thresholds as the local minima that bounded this peak. A region of interest (ROI) was defined in the center of the specimens as follows. A virtual cylinder (4 mm diameter) was defined in the middle of the dome extending from the base of the calvaria to the apex of the tissue. This site was targeted because it represented the central area where dental implants are likely to be placed following such regenerative procedure. The cylinder was then divided transversely into three parts – bottom, middle, and top – (Figure 1) in order to examine the effect of the distance from the original calvarium (that is the primary source of cells and vessels for new bone formation) on the

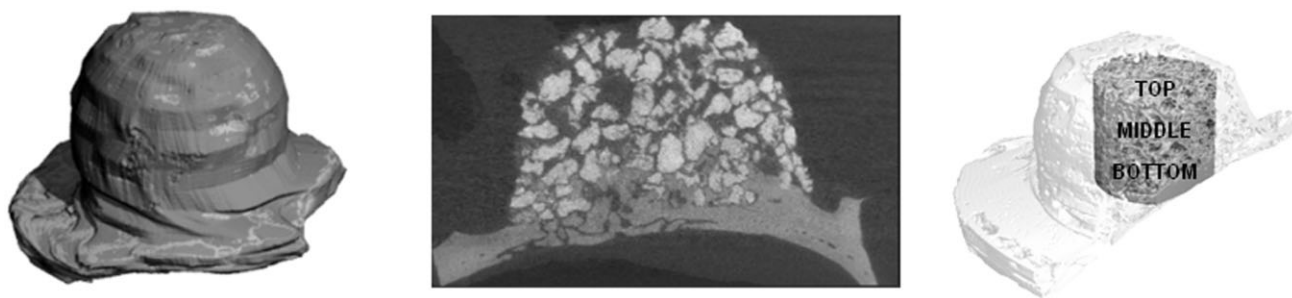


Figure 1 Representative μ CT rendering: dark gray – bone, white – TCP; entire specimen (left); sagittal cutaway view demonstrating that bone is the dominant component in the lower portion of the dome whereas TCP is more dominant in the upper portion (middle); diagrammatic presentation of the three subregions of the cylindrical ROI (right). μ CT = microcomputed tomography; ROI = region of interest; TCP = tricalcium phosphate.

extent of bone formation. The following parameters were calculated for the whole cylinder as well as the three subregions: bone volume fraction (BV/TV), tissue mineral density (TMD), and β TCP volume fraction.

Histological Preparations

NBF-fixed specimens were decalcified in Calci-Clear Rapid (National Diagnostic, Atlanta, GA, USA) for 2 to 3 days, cut in half at the midline, embedded in paraffin, and sectioned ($5\ \mu\text{m}$). For determination of bone morphology, sections were stained with hematoxylin and eosin.

Histomorphometric Analysis

Four stained sections ($\sim 20\ \mu\text{m}$ apart) from each specimen were captured by a digital camera (Olympus DP70) with a calibration scale and analyzed morphometrically using ImageJ software (NIH, Bethesda, MD, USA). Mean value was calculated for each specimen (from four measurements); later the mean \pm standard error (SE) was calculated for each group.

Two parameters were measured: (1) vertical bone height (VBH): maximal bone height (in millimeter) measured from the base of the calvarium to the crest of the newly formed bone and (2) bone fraction: percentage of the bone from the overall tissue under the dome. As the newly formed bone could not be separated from the original calvarium and as calvarium width is similar in all rats (average 0.8 mm), bone height, area, and percentage included the newly formed bone + the original calvarium.

Statistical Analysis

StatPlus® (AnalystSoft, Vancouver, BC, Canada) and JMP 10.0 (SAS Institute, Cary, NC, USA) statistical

packages were used. Descriptive statistics that included means and medians, ranges, and SE were initially tabulated. Comparisons between EPC and CNT groups for the measurements from the whole cylinder were performed using *t*-tests or Wilcoxon tests, depending on whether the variances were equal. Comparisons between EPC and CNT groups for the measurements from the cylindrical subregions were performed using two-factor repeated-measures analysis of variance (ANOVA) with subregion location as the within-subjects factor and treatment as the between-subjects factor. These ANOVAs tested whether the effect of cell transplantation differed intragroup comparisons of the volume fractions and TMDs were performed among the three parts of the cylinder (e.g., EPC BV/TV top vs EPC BV/TV middle vs EPC BV/TV bottom). Post hoc comparisons were made in a paired manner with Bonferroni correction. A significance level of $p < .05$ was used.

RESULTS

EPC Isolation, Expansion, and Characterization

EPCs were isolated and cultured as described in “Materials and Methods.” Immediately after seeding cells appeared rounded, but after 3 to 5 days, attached cells appeared to have changed their contour to a more polygonal shape. Cells rapidly replicated and formed a monolayer of homogenous appearance (Figure 2A). According to FACS analysis, EPCs were CD90⁺, CD44⁺, CD45⁻, CD31⁻, and CD34⁻ (see Figure 2B). EPCs that were cultured on Matrigel-coated plates formed cellular clusters 2 days following seeding. Moreover, tube formation was noted 5 days following seeding (see Figure 2A).

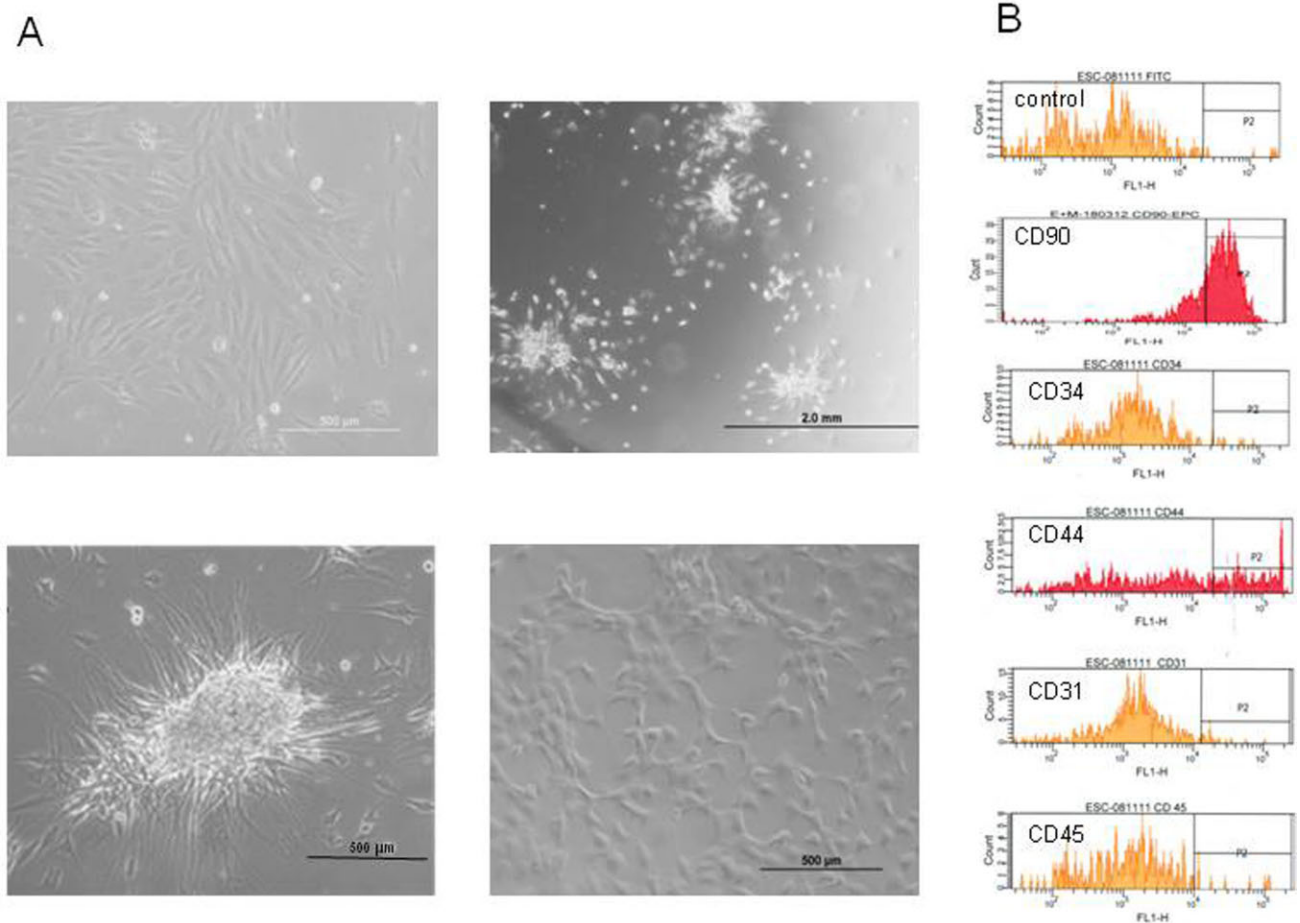


Figure 2 A, Peripheral blood endothelial progenitor cells (EPCs) isolated from rat: 9 days after isolation, EPC seeded on fibronectin presented polygonal shape (upper left, magnification $\times 10$). Two days after seeding on Matrigel, EPC formed clusters (upper right magnification $\times 4$). A higher magnification of a cluster revealed spindle-shaped cells that are radiated from a core of cellular aggregate (lower left, magnification $\times 10$). Five days after seeding on Matrigel, EPC formed tubes (lower right magnification $\times 10$). B, According to FACS analysis, EPCs were CD90⁺, CD44⁺, CD45⁻, CD31⁻, and CD34⁻.

Macroscopic View

All rats survived the surgical procedures. Healing was uneventful, and new augmented hard tissue formed in the space under the capsule.

μ CT Analysis

Analyses of the whole cylinder (Figure 3) showed that transplantation of EPC resulted in higher BV/TV compared with CNT rats ($38 \pm 1\%$ vs 32 ± 1 , $p = .0169$), while no difference in TMD was observed between groups (963 ± 3.8 mg HA/cm³ vs 966 ± 8.1 mg HA/cm³, $p = .796$). TCP volume fraction was also similar in both groups ($30 \pm 0.9\%$ vs 32 ± 1.0 , $p = .236$), suggesting a similar degradation rate of the scaffold. Analyses of the three different subregions of the cylinder revealed that both the distance from the original calvaria and the cell transplantation affected bone formation (Figure 4).

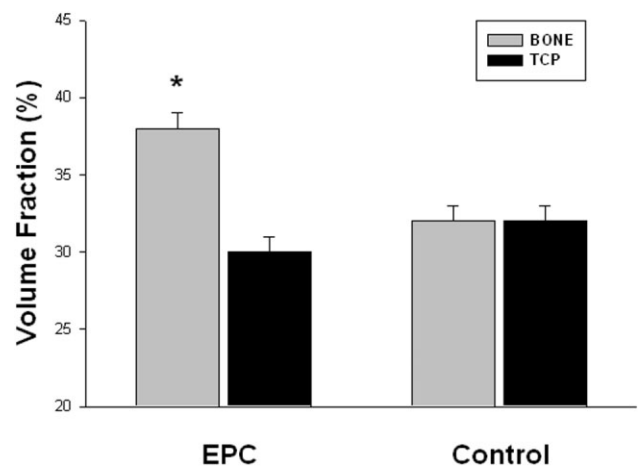


Figure 3 Bone volume fraction (BV/TV) and TCP: BV/TV (gray columns) was significantly higher in EPC group compared with CNT ($*p = .0169$). No difference in the volume fraction of TCP (black columns) was noted between the groups. CNT = control; EPC = endothelial progenitor cell; TCP = tricalcium phosphate.

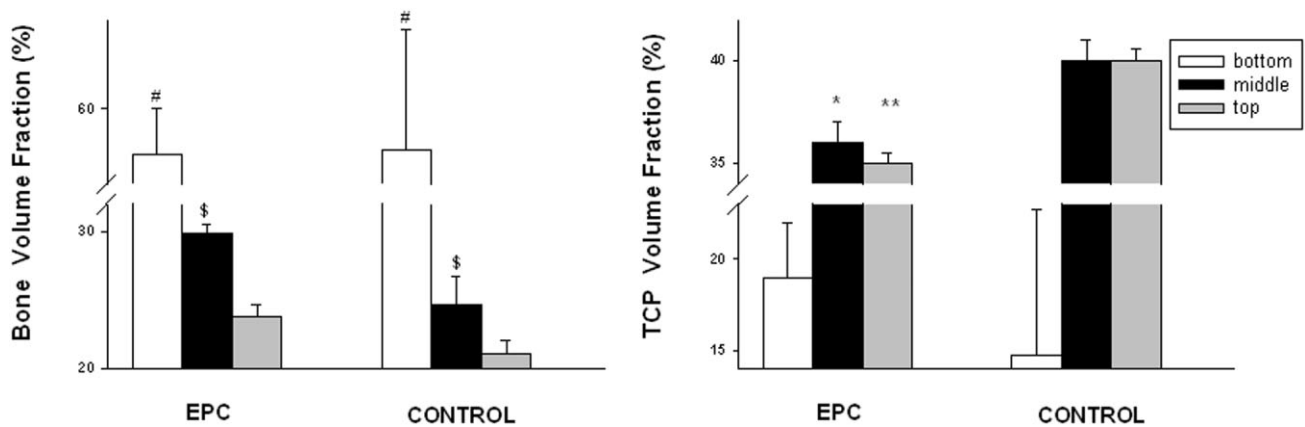


Figure 4 Bone and TCP volume fraction in the three subregions of the cylinder: bottom (white), middle (black), and top (gray); TCP volume fraction (right chart) intergroup comparison EPC versus CNT: *denotes $p \leq .005$, **denotes $p \leq .001$. Bone volume fraction (left chart) differences between subregions within each group: middle and top versus bottom # denotes $p < .0001$; top versus middle; \$ denotes significant differences $p < .0001$. CNT = control; EPC = endothelial progenitor cell; TCP = tricalcium phosphate.

In both EPC and CNT, BV/TV declined from bottom to the top of the cylinder ($p < .0001$). However, there was a trend toward an effect of cell transplantation on this rate of decline ($p = .0688$), which arose from elevated BV/TV values in the middle and top subregions in the EPC group compared with CNTs. Similarly, in the middle and top subregions, TCP volume fraction was lower in the EPC group compared with CNTs ($p \leq .005$).

Descriptive Histology and Histomorphometric Measurements

Histological sections revealed that the total volume of the augmented tissue was composed of bone, residual scaffold, and connective tissue. The proportions of these components were different between groups and within rats of the same group (Figure 5A–D). In the lower part of the specimens, newly formed mature lamellar bone was continuous with the original calvaria, indicative of more mature bone formation (see Figure 5E). However, the upper (distal) part of the augmented tissue contained residual scaffold surrounded by dense vascularized connective tissue (see Figure 5A–C).

Histomorphometric analyses revealed that all measured bone parameters were significantly higher in the EPC group compared with CNT group. All histomorphometric results are summarized in Figure 6. VBH was doubled by transplantation of EPC (EPC 4.04 ± 0.22 mm vs CNT 2.29 ± 0.22 mm, $p \leq .001$). In addition, transplantation of EPC caused ~50% increase in bone area fraction that was $47.3 \pm 3.1\%$ versus $31.1 \pm 2.7\%$, $p \leq .003$ in EPC versus CNT, respectively.

DISCUSSION

Vertical extra-cortical bone augmentation is a challenging task mainly due to “unfavorable” environmental conditions of poor cellular, nutrient, and blood supply. Furthermore, clinical demand for vertical bone augmentation is ever increasing as the use of dental implants has become extremely popular. This study introduces a new paradigm to enhance vertical bone formation by improving the environmental conditions. By combining GBR and EPC transplantation, we increased the population of available cells for bone regeneration in an established rat calvarium model.^{27–30} The results demonstrate significant enhancement of bone augmentation by EPC transplantation under a rigid gold dome. EPC transplantation produced a 5-mm increase in the height of newly formed hard tissue with a bone area fraction that was higher than 40%.

EPCs were isolated from the MNCs of rat peripheral blood. MNCs contain mainly hematopoietic cells and to lesser extent (<0.001%) stem or progenitor cells that migrated from the bm to the peripheral blood.³¹ Separating hematopoietic cells from stem/progenitor cells is based on the ability of stem/progenitor to adhere to plastic culture plates while hematopoietic cells consider as nonadherent cells.³² As our laboratory possesses extensive experience with isolation and culture of EPCs from peripheral blood,²⁴ we isolated and cultured the progenitor cells in the current study in conditions that advance EPC expansion.³³ Indeed, the behavior and morphology of EPC that were isolated corresponded with “late EPC” type: the attached cells appeared

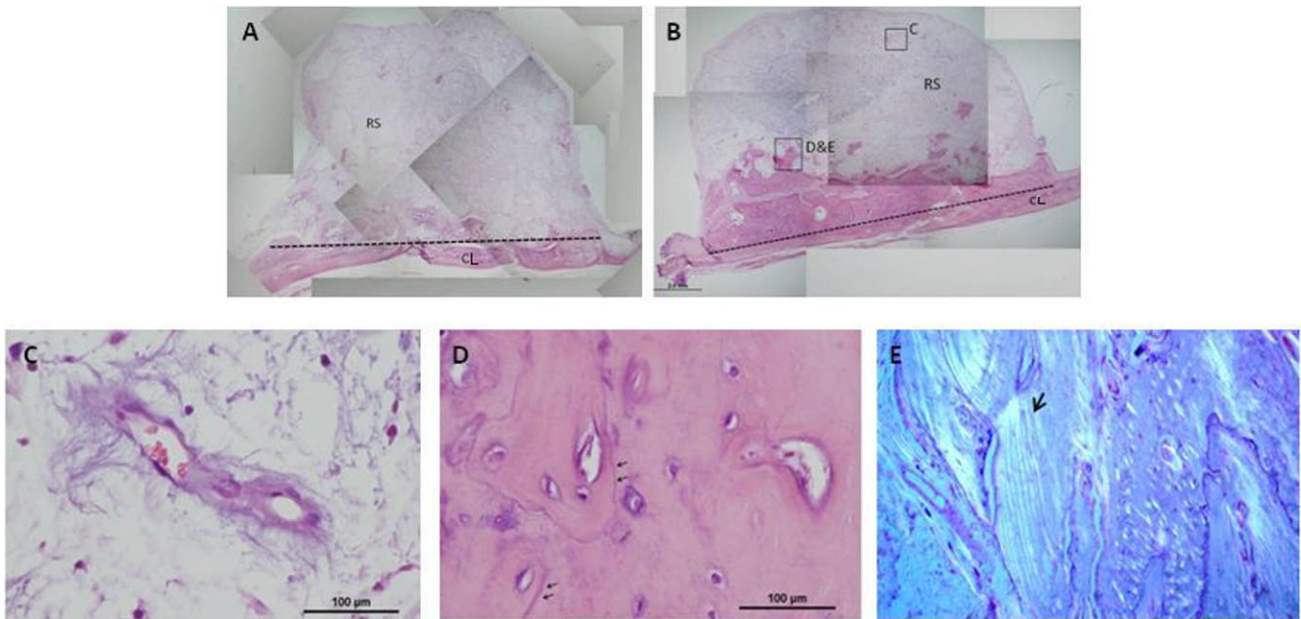


Figure 5 Representative (H&E) histological analysis of CNT and EPC transplanted groups. (A,B) Representative images of: CNT (A) and EPC (B). Newly formed tissue that filled the space under the gold dome is continuous with the original calvaria (CL). The dotted line demonstrates the upper border of the original calvaria. RS indicates residual scaffold. (C) Higher magnification of the upper rectangular region in B, showing a highly vascularized connective tissue in the distal part of the regenerated tissue. (D,E) Higher magnification of the lower rectangular in B; (D) reversal lines (black arrows) indicate bone remodeling in the newly formed bone. (E) Polarized light illumination exemplified more mature lamellar bone (magnification $\times 4$). CNT = control; EPC = endothelial progenitor cell; H&E = hematoxylin and eosin.

polygonal, rapidly replicated, and formed a monolayer of homogenous appearance.^{22,23,34,35} Moreover, when EPCs were cultured on Matrigel, cluster formation and tube formation appeared as described by Asahara and colleagues.¹⁹ Nevertheless, the antigenic phenotype of rat's EPC lacked endothelial and hematopoietic characteristics (rat's EPCs were negative to CD31, CD34, and

CD45), but 90 and 40% of cells were positive to CD90 and CD44, respectively, which are surface antigens that characterize MSC.³⁶ The explanation to our inconsistent antigenic phenotype and cell's morphology could be the characterization of a common progenitor for endothelial and mesodermal in culture that termed mesoangioblasts.^{37,38} Furthermore, it is also possible that species

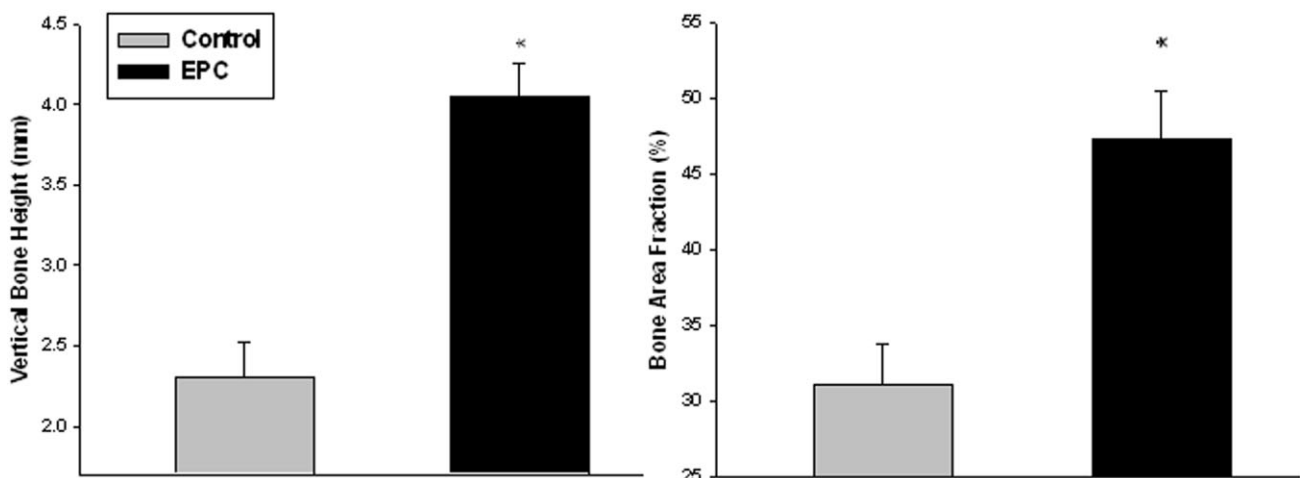


Figure 6 Histomorphometric analyses of vertical bone height (millimeter) and bone area fraction (percent). * $p \leq .05$, EPC versus CNT. CNT = control; EPC = endothelial progenitor cell.

specificity might explain the difference in antigenicity between the cells.³⁹

Histological slides and histomorphometric analyses showed mature lamellar bone extending from the original calvaria and partially filled the space under the rigid dome. Significantly higher measurements for all bone parameters were obtained when EPCs were transplanted compared with CNT (β TCP). Likewise, in our previous study,²⁸ in a similar experimental model, transplantation of 5×10^5 bm MSC under a rigid dome significantly improved vertical bone formation. The addition of osteogenic transformed (ot) MSC has resulted in a significantly higher proportions of new bone ($47.21 \pm 2.49\%$) compared with bm MSC ($37.34 \pm 3.31\%$). Comparing the results of the current and previous studies, it can be concluded that vertical bone augmentation with the addition of EPC transplantation was superior to bm MSC and equivalent to ot MSC transplantation. In accordance with our results, Pieri and colleagues²⁹ seeded adipose-derived MSC mixed with xenograft scaffold under titanium domes fixed to a rabbit calvarium. Vertical bone formation was tested using 10^5 to 10^7 cells. The best results of 3 mm of VBH were achieved by transplantation of 10^7 cells.²⁹ From a clinical point of view, the isolation of cells from the peripheral blood is favored over bm or adipose aspiration, as it involves minimal morbidity and is more “patient friendly.”

The major advantages of μ CT include three-dimensional analysis of the quantity and mineral density of both bone and scaffold. Differences in mineral density between bone (~ 960 mg HA/cm³) and TCP (~ 1650 mg HA/cm³) allowed us to separate these two components in the analysis. μ CT analysis was performed for a cylindrical core sample that was defined as the ROI in the middle of the dome that corresponds to the desired location of dental implant in cases where bone augmentation is performed to allow for implant placement. This ROI was further divided into three subregions: bottom, middle, and top. BV/TV was highest in the bottom, moderate in the middle, and lowest in the top of the cylinder in both CNT and EPC groups. This is similar to the healing pattern following teeth extraction and bone fracture in which bone regeneration originates from the preexisting bone.^{40,41} These results are logical as blood, cells, and nutrient supply that are necessary for bone growth originate from the calvarium and gradually decrease toward the top of the dome. However, the present results also

indicate that while the contribution of GBR and β TCP to vertical bone formation is largely limited to the area adjacent to the original calvarium, EPC transplantation promoted bone formation in more remote areas (i.e., the middle and top parts of the cylinder). These findings suggest that the limiting factor for vertical bone augmentation in this GBR model is the amount of osteoprogenitor cells and that this limiting factor was partially overcome by the addition of EPCs.

Although the present study was performed in the rat, not human, rat calvarium is an acceptable model to test vertical extra-cortical bone formation in small animals as the calvarium and jaw are formed through intramembranous bone formation.⁴² As the limitations of the present study are primarily associated with the use of a rat cells, future studies will be dedicated to explore vertical bone formation using human cells in nude rat calvarium.

CONCLUSIONS

EPC transplantation improved bone formation especially in the areas that are remote from the original bone.

ACKNOWLEDGMENTS

We would like to thank Dr. Margarita Filatov and Shami Ivanka for FACS analysis and Mr. Gabriel McDonald and Mr. Benjamin Pritz for μ CT analysis.

Sources of Funding: Ministry of Industry Trade and Labor, Israel Government – Kamin No. 46293; Ofakim grant, Rambam Health Care Campus, Haifa, Israel.

REFERENCES

1. Keller EE, Triplett WW. Iliac bone grafting: review of 160 consecutive cases. *J Oral Maxillofac Surg* 1987; 45:11–14.
2. Waasdorp J, Reynolds MA. Allogeneic bone onlay grafts for alveolar ridge augmentation: a systematic review. *Int J Oral Maxillofac Implants* 2010; 25:525–531.
3. Zerbo IR, de Lange GL, Joldersma M, Bronckers AL, Burger EH. Fate of monocortical bone blocks grafted in the human maxilla: a histological and histomorphometric study. *Clin Oral Implants Res* 2003; 14:759–766.
4. Kim CS, Choi SH, Chai JK, et al. Periodontal repair in surgically created intrabony defects in dogs: influence of the number of bone walls on healing response. *J Periodontol* 2004; 75:229–235.
5. Chiapasco M, Abati S, Romeo E, Vogel G. Clinical outcome of autogenous bone blocks or guided bone regeneration with e-PTFE membranes for the reconstruction of narrow edentulous ridges. *Clin Oral Implants Res* 1999; 10:278–288.

6. Simion M, Jovanovic SA, Tinti C, Benfenati SP. Long-term evaluation of osseointegrated implants inserted at the time or after vertical ridge augmentation. A retrospective study on 123 implants with 1–5 year follow-up. *Clin Oral Implants Res* 2001; 12:35–45.
7. Esposito M, Grusovin MG, Coulthard P, Worthington HV. The efficacy of various bone augmentation procedures for dental implants: a Cochrane systematic review of randomized controlled clinical trials. *Int J Oral Maxillofac Implants* 2006; 21:696–710.
8. Khosla S, Westendorf JJ, Mödder UI. Concise review: insights from normal bone remodeling and stem cell-based therapies for bone repair. *Stem Cells* 2010; 28:2124–2128.
9. Ward BB, Brown SE, Krebsbach PH. Bioengineering strategies for regeneration of craniofacial bone: a review of emerging technologies. *Oral Dis* 2010; 16:709–716.
10. Kaigler D, Pagni G, Park CH, Tarle SA, Bartel RL, Giannobile WV. Angiogenic and osteogenic potential of bone repair cells for craniofacial regeneration. *Tissue Eng Part A* 2010; 16:2809–2820.
11. Friedenstein AJ, Piatetzky-Shapiro II, Petrakova KV. Osteogenesis in transplants of bone marrow cells. *J Embryol Exp Morphol* 1966; 16:381–390.
12. Deschaseaux F, Pontikoglou C, Sensébé L. Bone regeneration: the stem/progenitor cells point of view. *J Cell Mol Med* 2010; 14:103–115.
13. Petite H, Viateau V, Bensaïd W, et al. Tissue-engineered bone regeneration. *Nat Biotechnol* 2000; 18:959–963.
14. Bruder SP, Kraus KH, Goldberg VM, et al. The effect of implants loaded with autologous mesenchymal stem cells on the healing of canine segmental bone defects. *J Bone Joint Surg Am* 1998; 80:985–996.
15. Quarto R, Mastrogiacomo M, Cancedda R, et al. Repair of large bone defects with the use of autologous bone marrow stromal cells. *N Engl J Med* 2001; 344:385–386.
16. Horwitz EM, Prockop DJ, Fitzpatrick LA, et al. Transplantability and therapeutic effects of bone marrow-derived mesenchymal cells in children with osteogenesis imperfecta. *Nat Med* 1999; 5:309–313.
17. Sauerbier S, Rickert D, Gutwald R, et al. Bone marrow concentrate and bovine bone mineral for sinus floor augmentation: a controlled, randomized, single-blinded clinical and histological trial – per-protocol analysis. *Tissue Eng Part A* 2011; 17:2187–2197.
18. Kuznetsov SA, Mankani MH, Gronthos S, Satomura K, Bianco P, Robey PG. Circulating skeletal stem cells. *J Cell Biol* 2001; 153:1133–1140.
19. Asahara T, Murohara T, Sullivan A, et al. Isolation of putative progenitor endothelial cells for angiogenesis. *Science* 1997; 275:964–967.
20. Gössl M, Mödder UI, Atkinson EJ, Lerman A, Khosla S. Osteocalcin expression by circulating endothelial progenitor cells in patients with coronary atherosclerosis. *J Am Coll Cardiol* 2008; 52:1314–1325.
21. Luttun A, Carmeliet G, Carmeliet P. Vascular progenitors: from biology to treatment. *Trends Cardiovasc Med* 2002; 12:88–96.
22. Fuchs S, Ghanaati S, Orth C, et al. Contribution of outgrowth endothelial cells from human peripheral blood on in vivo vascularization of bone tissue engineered constructs based on starch polycaprolactone scaffolds. *Biomaterials* 2009; 30:526–534.
23. Hur J, Yoon CH, Kim HS, et al. Characterization of two types of endothelial progenitor cells and their different contributions to neovascularization. *Arterioscler Thromb Vasc Biol* 2004; 24:288–293.
24. Rozen N, Bick T, Bajayo A, et al. Transplanted blood-derived endothelial progenitor cells (EPC) enhance bridging of sheep tibia critical size defects. *Bone* 2009; 45:918–924.
25. Seebach C, Henrich D, Kähling C, et al. Endothelial progenitor cells and mesenchymal stem cells seeded onto beta-TCP granules enhance early vascularization and bone healing in a critical-sized bone defect in rats. *Tissue Eng Part A* 2010; 16:1961–1970.
26. Atesok K, Li R, Stewart DJ, Schemitsch EH. Endothelial progenitor cells promote fracture healing in a segmental bone defect model. *J Orthop Res* 2010; 28:1007–1014.
27. Zigdon H, Lewinson D, Bick T, Machtei EE. Vertical bone augmentation using different osteoconductive scaffolds combined with barrier domes in the rat calvarium. *Clin Implant Dent Relat Res* 2012. doi: 10.1111/j.1708-8208.2012.00452.10
28. Zigdon H, Lewinson D, Bick T, Machtei EE. Mesenchymal stem cells combined with barrier domes enhance vertical bone formation. *J Clin Periodontol* 2013; 40:196–202.
29. Pieri F, Lucarelli E, Corinaldesi G, et al. Dose-dependent effect of adipose-derived adult stem cells on vertical bone regeneration in rabbit calvarium. *Biomaterials* 2010; 31:3527–3535.
30. Lundgren D, Lundgren AK, Sennerby L, Nyman S. Augmentation of intramembraneous bone beyond the skeletal envelope using an occlusive titanium barrier. An experimental study in the rabbit. *Clin Oral Implants Res* 1995; 6:67–72.
31. Dazzi F, Ramasamy R, Glennie S, Jones SP, Roberts I. The role of mesenchymal stem cells in haemopoiesis. *Blood Rev* 2006; 20:161–171.
32. Friedenstein AJ, Chailakhjan RK, Lalykina KS. The development of fibroblast colonies in monolayer cultures of guinea-pig bone marrow and spleen cells. *Cell Tissue Kinet* 1970; 3:393–403.
33. Ingram DA, Mead LE, Tanaka H, et al. Identification of a novel hierarchy of endothelial progenitor cells using human peripheral and umbilical cord blood. *Blood* 2004; 104:2752–2760.

34. Yoder MC, Mead LE, Prater D, et al. Redefining endothelial progenitor cells via clonal analysis and hematopoietic stem/progenitor cell principals. *Blood* 2007; 109:1801–1809.
35. Hirschi KK, Ingram DA, Yoder MC. Assessing identity, phenotype, and fate of endothelial progenitor cells. *Arterioscler Thromb Vasc Biol* 2008; 28:1584–1595.
36. Nery AA, Nascimento IC, Glaser T, Bassaneze V, Krieger JE, Ulrich H. Human mesenchymal stem cells: from immunophenotyping by flow cytometry to clinical applications. *Cytometry A* 2013; 83:48–61.
37. Minasi MG, Riminucci M, De Angelis L, et al. The mesoangioblast: a multipotent, self-renewing cell that originates from the dorsal aorta and differentiates into most mesodermal tissues. *Development* 2002; 129:2773–2783.
38. Cossu G, Bianco P. Mesoangioblasts-vascular progenitors for extravascular mesodermal tissues. *Curr Opin Genet Dev* 2003; 13:537–542.
39. Yang N, Li D, Jiao P, et al. The characteristics of endothelial progenitor cells derived from mononuclear cells of rat bone marrow in different culture conditions. *Cytotechnology* 2011; 63:217–226.
40. Artzi Z, Tal H, Dayan D. Porous bovine bone mineral in healing of human extraction sockets: 2. Histochemical observations at 9 months. *J Periodontol* 2001; 72:152–159.
41. Rozen N, Lewinson D, Bick T, Meretyk S, Soudry M. Role of bone regeneration and turnover modulators in control of fracture. *Crit Rev Eukaryot Gene Expr* 2007; 17: 197–213.
42. Verna C, Dalstra M, Wikesjö UM, Trombelli L, Bosch C. Healing patterns in calvarial bone defects following guided bone regeneration in rats. A micro-CT scan analysis. *J Clin Periodontol* 2002; 29:865–870.

Copyright of Clinical Implant Dentistry & Related Research is the property of Wiley-Blackwell and its content may not be copied or emailed to multiple sites or posted to a listserv without the copyright holder's express written permission. However, users may print, download, or email articles for individual use.